



IJRASET

International Journal For Research in
Applied Science and Engineering Technology



INTERNATIONAL JOURNAL FOR RESEARCH

IN APPLIED SCIENCE & ENGINEERING TECHNOLOGY

Volume: 10 **Issue:** XI **Month of publication:** November 2022

DOI: <https://doi.org/10.22214/ijraset.2022.47321>

www.ijraset.com

Call:  08813907089

E-mail ID: ijraset@gmail.com

Spectroscopic Properties of Er^{3+} Doped in Zinc Lithium Calcium Potassiumniobate Phosphate Glasses

Pankaj Deedwaniya¹, S. L. Meena²

^{1,2}Ceramic Laboratory, Department of physics, Jai Narain Vyas University, Jodhpur 342001(Raj) India

Abstract: Zinc lithium calcium potassiumniobate phosphate glasses containing Er^{3+} in (45-x): $\text{P}_2\text{O}_5:10\text{ZnO}:10\text{Li}_2\text{O}:10\text{CaO}:10\text{K}_2\text{O}:15\text{Nb}_2\text{O}_5:x\text{Er}_2\text{O}_3$, (where $x=1, 1.5, 2$ mol %) have been prepared by melt-quenching method. The amorphous nature of the glasses was confirmed by x-ray diffraction studies. Optical absorption, Excitation, and fluorescence spectra were recorded at room temperature for all glass samples. Judd-Ofelt intensity parameters Ω_λ ($\lambda=2, 4, 6$) are evaluated from the intensities of various absorption bands of optical absorption spectra. Using these intensity parameters various radiative properties like spontaneous emission probability, branching ratio, radiative life time and stimulated emission cross-section of various emission lines have been evaluated.

Keywords: ZLCPNP Glasses, Optical Properties, Judd-Ofelt Theory.

I. INTRODUCTION

Rare-earth ions doped glass-ceramics are important materials for optical fibers, wave guide lasers, sensors and optical amplifiers [1-5]. Oxide glasses are the most stable host matrices for practical applications due to their high chemical durability and thermal stability [6-10]. Phosphate glasses are extremely attractive materials for linear and non-linear application in optics, due to their important aspects such as their low melting temperature, low phonon energy, high refractive index, high dielectric constant, good chemical durability, high thermal stability, good solubility of rare earth ions [11-16]. The addition of heavy metal oxide to phosphate glasses decreases the phonon energy. Thus, leads to increase in its quantum efficiency of luminescence from the excited state of rare earth ions. Er^{3+} doped rare earth doped glasses considerable literature has recently emerged concerning the structure, optical, mechanical, thermal, and electrical properties [17-20].

In this work, the spectroscopic properties of Er^{3+} -doped (45-x): $\text{P}_2\text{O}_5:10\text{ZnO}:10\text{Li}_2\text{O}:10\text{CaO}:10\text{K}_2\text{O}:15\text{Nb}_2\text{O}_5:x\text{Er}_2\text{O}_3$ (where $x=1, 1.5, 2$ mol %) glasses were investigated. The Optical absorption, Excitation and fluorescence spectra of Er^{3+} of the glasses were investigated. The intensities of the transitions for the rare earth ions have been estimated successfully using the Judd-Ofelt theory. The laser parameters such as radiative probabilities (A), branching ratio (β), radiative life time (τ_R) and stimulated emission cross section (σ_p) are evaluated using J.O. intensity parameters (Ω_λ , $\lambda=2, 4$ and 6).

II. EXPERIMENTAL TECHNIQUES

A. Preparation of Glasses

The following Er^{3+} doped zinc lithium calcium potassiumniobate phosphate glass samples (45-x): $\text{P}_2\text{O}_5:10\text{ZnO}:10\text{Li}_2\text{O}:10\text{CaO}:10\text{K}_2\text{O}:15\text{Nb}_2\text{O}_5:x\text{Er}_2\text{O}_3$ (where $x=1, 1.5, 2$) have been prepared by melt-quenching method. Analytical reagent grade chemical used in the present study consist of P_2O_5 , ZnO, Li_2O , CaO, K_2O , Nb_2O_5 and Er_2O_3 . All weighed chemicals were powdered by using an Agate pestle mortar and mixed thoroughly before each batch (10g) was melted in alumina crucibles in silicon carbide based an electrical furnace.

Silicon Carbide Muffle furnace was heated to working temperature of 1070°C , for preparation of zinc lithium calcium potassiumniobate phosphate glasses, for two hours to ensure the melt to be free from gases. The melt was stirred several times to ensure homogeneity. For quenching, the melt was quickly poured on the steel plate & was immediately inserted in the muffle furnace for annealing. The steel plate was preheated to 100°C . While pouring; the temperature of crucible was also maintained to prevent crystallization. And annealed at temperature of 350°C for 2h to remove thermal strains and stresses. Every time fine powder of cerium oxide was used for polishing the samples. The glass samples so prepared were of good optical quality and were transparent. The chemical compositions of the glasses with the name of samples are summarized in Table 1

Table 1 Chemical composition of the glasses

Sample	Glass composition (mol %)
ZLCPNP (UD)	45 P ₂ O ₅ :10ZnO:10Li ₂ O:10CaO:10K ₂ O:15Nb ₂ O ₅
ZLCPNP (ER 1)	44 P ₂ O ₅ :10ZnO:10Li ₂ O:10CaO:10K ₂ O:15Nb ₂ O ₅ :1 Er ₂ O ₃
ZLCPNP (ER 1.5)	43.5 P ₂ O ₅ :10ZnO:10Li ₂ O:10CaO:10K ₂ O:15Nb ₂ O ₅ :1.5 Er ₂ O ₃
ZLCPNP (ER 2)	43 P ₂ O ₅ :10ZnO:10Li ₂ O:10CaO:10K ₂ O:15Nb ₂ O ₅ : 2 Er ₂ O ₃

ZLCPNP (UD)—Represents undoped Zinc Lithium Calcium Potassiumniobate phosphate glass specimen.
 ZLCPNP (ER) -Represents Er³⁺ doped Zinc Lithium Calcium Potassiumniobate phosphate glass specimens.

III. THEORY

A. Oscillator Strength

The intensity of spectral lines are expressed in terms of oscillator strengths using the relation [21].

$$f_{\text{expt.}} = 4.318 \times 10^{-9} [\epsilon(v) d v] \quad (1)$$

where, $\epsilon(v)$ is molar absorption coefficient at a given energy v (cm⁻¹), to be evaluated from Beer–Lambert law.

Under Gaussian Approximation, using Beer–Lambert law, the observed oscillator strengths of the absorption bands have been experimentally calculated, using the modified relation [22].

$$P_m = 4.6 \times 10^{-9} \times \frac{1}{cl} \log \frac{I_0}{I} \times \Delta v_{1/2} \quad (2)$$

where c is the molar concentration of the absorbing ion per unit volume, l is the optical path length, $\log I_0/I$ is absorbivity or optical density and $\Delta v_{1/2}$ is half band width.

B. Judd-Ofelt Intensity Parameters

According to Judd [23] and Ofelt [24] theory, independently derived expression for the oscillator strength of the induced forced electric dipole transitions between an initial J manifold $|4f^N(S, L) J\rangle$ level and the terminal J' manifold $|4f^N(S', L') J'\rangle$ is given by:

$$\frac{8\pi^2 m c \bar{\nu}}{3h(2J+1)n} \frac{1}{n} \left[\frac{(n^2+2)^2}{9} \right] \times S(J, J') \quad \text{where,} \quad (3)$$

the line strength $S(J, J')$ is given by the equation

$$S(J, J') = e^2 \sum_{\lambda=2, 4, 6} \Omega_{\lambda} \langle 4f^N(S, L) J || U^{(\lambda)} || 4f^N(S', L') J' \rangle^2 \quad (4)$$

In the above equation m is the mass of an electron, c is the velocity of light, $\bar{\nu}$ is the wave number of the transition, h is Planck's constant, n is the refractive index, J and J' are the total angular momentum of the initial and final level respectively, Ω_{λ} ($\lambda = 2, 4$ and 6) are known as Judd-Ofelt intensity parameters.

C. Radiative Properties

The Ω_{λ} parameters obtained using the absorption spectral results have been used to predict radiative properties such as spontaneous emission probability (A) and radiative life time (τ_R), and laser parameters like fluorescence branching ratio (β_R) and stimulated emission cross section (σ_p).

The spontaneous emission probability from initial manifold $|4f^N(S', L') J'\rangle$ to a final manifold $|4f^N(S, L) J\rangle$ is given by:

$$A[(S', L') J'; (S, L) J] = \frac{64 \pi^2 \bar{\nu}^3}{3h(2J'+1)} \left[\frac{n(n^2+2)^2}{9} \right] \times S(J', J) \quad (5)$$

Where, $S(J, J') = e^2 [\Omega_2 || U^{(2)} ||^2 + \Omega_4 || U^{(4)} ||^2 + \Omega_6 || U^{(6)} ||^2]$

The fluorescence branching ratio for the transitions originating from a specific initial manifold $|4f^N(S', L') J'\rangle$ to a final manifold $|4f^N(S, L) J\rangle$ is given by

$$\beta[(S', L') J'; (S, L) J] = \sum_{S L J} \frac{A[(S' L) J']}{A[(S' L') J' (S L) J]} \quad (6)$$

where, the sum is over all terminal manifolds.

The radiative life time is given by

$$\tau_{rad} = \sum_{S, L, J} A[(S', L') J'; (S, L) J] = A_{Total}^{-1} \tag{7}$$

where, the sum is over all possible terminal manifolds. The stimulated emission cross-section for a transition from an initial manifold $|4f^N(S', L') J\rangle$ to a final manifold $|4f^N(S, L) J\rangle$ is expressed as

$$\sigma_p(\lambda_p) = \left[\frac{\lambda_p^4}{8\pi c n^2 \Delta\lambda_{eff}} \right] \times A[(S', L') J'; (\bar{S}, \bar{L}) \bar{J}] \tag{8}$$

where, λ_p the peak fluorescence wavelength of the emission band and $\Delta\lambda_{eff}$ is the effective fluorescence line width.

D. Nephelauxetic Ratio (β') and Bonding Parameter ($b^{1/2}$)

The nature of the R-O bond is known by the Nephelauxetic Ratio (β') and Bonding Parameters ($b^{1/2}$), which are computed by using following formulae [25, 26]. The Nephelauxetic Ratio is given by

$$\beta' = \frac{v_g}{v_a} \tag{9}$$

where, v_a and v_g refer to the energies of the corresponding transition in the glass and free ion, respectively. The value of bonding parameter ($b^{1/2}$) is given by

$$b^{1/2} = \left[\frac{1 - \beta'}{2} \right]^{1/2} \tag{10}$$

IV. RESULT AND DISCUSSION

A. XRD Measurement

Figure 1 presents the XRD pattern of the samples containing show no sharp Bragg's peak, but only a broad diffuse hump around low angle region. This is the clear indication of amorphous nature with in the resolution limit of XRD instrument.

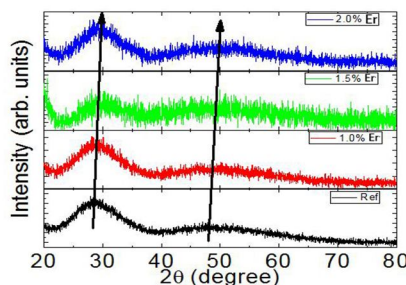


Fig.1: X-ray diffraction pattern of ZLCPNP (ER) glasses.

B. Absorption Spectra

The absorption spectra of ZLCPNP ER(01) glass, consists of absorption bands corresponding to the absorptions from the ground state $^4I_{15/2}$ of Er^{3+} ions. Ten absorption bands have been observed from the ground state $^4I_{15/2}$ to excited states $^4I_{11/2}$, $^4I_{9/2}$, $^4F_{9/2}$, $^4S_{3/2}$, $^2H_{11/2}$, $^4F_{7/2}$, $^4F_{5/2}$, $^4F_{3/2}$, $^2H_{9/2}$ and $^4G_{11/2}$ for Er^{3+} doped ZLCPNP ER (01) glass.

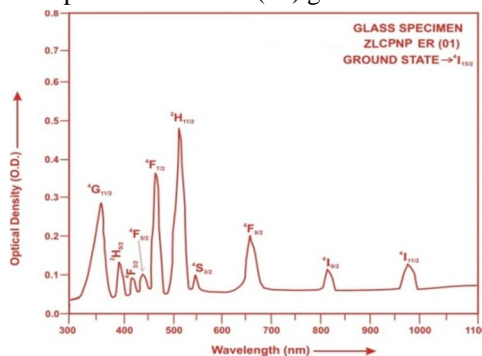


Fig.2: Absorption spectra of ZLCPNP ER (01) glass.

The experimental and calculated oscillator strengths for Er³⁺ ions in zinc lithium calcium potassium niobate phosphate glasses are given in Table 2

Table 2. Measured and calculated oscillator strength (P^m × 10⁺⁶) of Er³⁺ ions in ZLCPNP glasses.

Energy level ⁴ I _{15/2}	Glass ZLCPNP (ER01)		Glass ZLCPNP (ER1.5)		Glass ZLCPNP (ER02)	
	P _{exp.}	P _{cal.}	P _{exp.}	P _{cal.}	P _{exp.}	P _{cal.}
⁴ I _{11/2}	0.88	0.68	0.86	0.69	0.83	0.68
⁴ I _{9/2}	0.48	0.16	0.45	0.15	0.43	0.15
⁴ F _{9/2}	2.48	1.52	2.42	1.49	2.40	1.49
⁴ S _{3/2}	0.35	0.62	0.33	0.62	0.31	0.62
² H _{11/2}	6.45	2.36	6.42	2.37	6.39	2.37
⁴ F _{7/2}	5.36	2.17	5.33	2.17	5.30	2.16
⁴ F _{5/2}	0.62	0.79	0.64	0.79	0.62	0.79
⁴ F _{3/2}	0.30	0.48	0.27	0.49	0.25	0.48
² H _{9/2}	1.65	0.93	1.62	0.93	1.59	0.93
⁴ G _{11/2}	4.85	6.79	4.82	6.80	4.78	6.79
R.m.s.deviation	1.7993		1.7862		1.7778	

The various energy interaction parameters like Slater-Condon parameters F_k (k=2, 4, 6), Lande' parameter (ξ_{4f}) and Racah parameters E^k (k=1, 2, 3) have been computed using partial regression. Computed values of Slater-Condon, Lande', Racah, nephelauxetic ratio and bonding parameter for Er³⁺ doped ZLCPNP glass specimens are given in Table 3.

Table3. Computed values of Slater-Condon, Lande', Racah, nephelauxetic ratio and bonding parameter for Er³⁺ doped ZLCPNP glass specimens.

Parameter	Free ion	ZLCPNP ER01	ZLCPNP ER1.5	ZLCPNP ER02
F ₂ (cm ⁻¹)	441.680	433.883	433.874	433.894
F ₄ (cm ⁻¹)	68.327	67.048	67.0604	67.0363
F ₆ (cm ⁻¹)	7.490	7.0395	7.0401	7.0408
ξ _{4f} (cm ⁻¹)	2369.400	2414.822	2414.745	2415.158
E ¹ (cm ⁻¹)	6855.300	6661.445	6661.832	6661.517
E ² (cm ⁻¹)	32.126	31.335	31.3304	31.3411
E ³ (cm ⁻¹)	645.570	643.699	643.694	643.657
F ₄ /F ₂	0.15470	0.15453	0.15456	0.154499
F ₆ /F ₂	0.01696	0.016225	0.016226	0.0162271
E ¹ /E ³	10.61899	10.34869	10.34937	10.34948
E ² /E ³	0.049764	0.048680	0.048673	0.0486923
β'			.99567274	.99579898
b ^{1/2}			0.046514838	0.045831333

Judd-Ofelt intensity parameters Ω_λ (λ = 2, 4 and 6) were calculated by using the fitting approximation of the experimental oscillator strengths to the calculated oscillator strengths with respect to their electric dipole contributions. In the present case the three Ω_λ parameters follow the trend Ω₄ < Ω₂ < Ω₆.

The values of Judd-Ofelt intensity parameters are given in Table 4.

Table 4. Judd-Ofelt intensity parameters for Er³⁺ doped ZLCPNP glass specimens.

Glass Specimen	Ω ₂ (pm ²)	Ω ₄ (pm ²)	Ω ₆ (pm ²)	Ω ₄ /Ω ₆
ZLCPNP (ER01)	0.7970	0.3380	0.9525	0.3549
ZLCPNP (ER1.5)	0.8171	0.3102	0.9580	0.3238
ZLCPNP (ER02)	0.8134	0.3142	0.9516	0.3302

C. Excitation Spectrum

The Excitation spectra of Er³⁺ doped ZLCPNP glass specimens have been presented in Figure 3 in terms of Excitation Intensity versus wavelength. The excitation spectrum was recorded in the spectral region 300–600 nm fluorescence at 550nm having different excitation band centered at 350,365, 381, 425, 450, 470and 515 nm are attributed to the ²K_{15/2}, ⁴G_{9/2}, ⁴G_{11/2}, ²G_{9/2}, ⁴F_{3/2}, ⁴F_{5/2} and ²H_{11/2} transitions, respectively. The highest absorption level is ⁴G_{11/2} and is at 381nm. So this is to be chosen for excitation wavelength

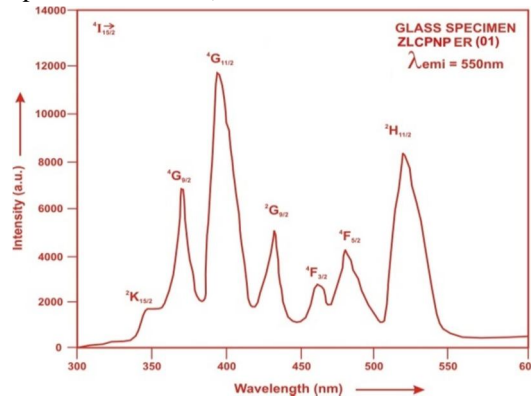


Fig.3: Excitation Spectrum of ZLCPNP ER (01) glass.

D. Fluorescence Spectrum

The fluorescence spectrum of Er³⁺ doped in zinc lithium calcium potassiumniobate phosphate glass is shown in Figure 4. There are four broad bands (⁴F_{7/2}→⁴I_{15/2}), (²H_{11/2}→⁴I_{15/2}), (⁴S_{3/2}→⁴I_{15/2}) and (⁴F_{9/2}→⁴I_{15/2}), respectively for glass specimens.

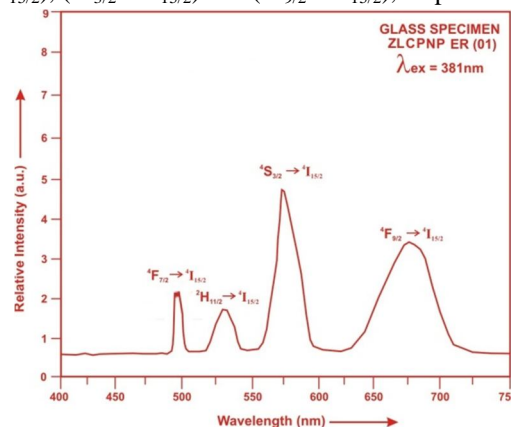


Fig.4: Fluorescence spectrum of ZLCPNP ER (01) glass.

Table 5. Emission peak wave lengths (λ_p), radiative transition probability (A_{rad}), branching ratio (β_R), stimulated emission crosssection (σ_p), and radiative life time (τ) for various transitions in Er³⁺ doped ZLCPNP glasses.

Transition	ZLCPNP ER 01					ZLCPNP ER 1.5					ZLCPNP ER 02			
	λ_{max} (nm)	$A_{rad}(s^{-1})$	β	σ_p ($10^{-20} cm^2$)	$\tau_R(\mu s)$	$A_{rad}(s^{-1})$	β	σ_p ($10^{-20} cm^2$)	τ_R (μs)	$A_{rad}(s^{-1})$	β	σ_p ($10^{-20} cm^2$)	τ_R ($10^{-20} cm^2$)	
⁴ F _{7/2} → ⁴ I _{15/2}	485	2090.68	0.4295	0.5212	205.4	2090.2	0.4275	0.5071	204.5	2085.42	0.4273	0.4918	204.91	
² H _{11/2} → ⁴ I _{15/2}	530	1223.23	0.2513	0.3639		1249.0	0.2555	0.3604		4	1248.80	0.2559		0.3521
⁴ S _{3/2} → ⁴ I _{15/2}	550	918.19	0.1886	0.2639		925.35	0.1893	0.2557			920.89	0.1887		0.2482
⁴ F _{9/2} → ⁴ I _{15/2}	657	635.95	0.1306	0.3212		624.34	0.1277	0.3081			625.19	0.1281		0.3031

V. CONCLUSION

In the present study, the glass samples of composition (45-x): $P_2O_5:10ZnO:10Li_2O:10CaO:10K_2O:15Nb_2O_5:xEr_2O_3$ (where $x = 1, 1.5, 2$ mol %) have been prepared by melt-quenching method. The value of stimulated emission cross-section (σ_p) is found to be maximum for the transition ($^4F_{7/2} \rightarrow ^4I_{15/2}$) for glass ZLCPNP (ER 01), suggesting that glass ZLCPNP (ER 01) is better compared to the other two glass systems ZLCPNP (ER1.5) and ZLCPNP (ER02).

REFERENCES

- [1] David L Veasey, David S Funk, Philip M peters, Norman A Sanford, Gregory P Peskin, Wei- Chin Liu, SN Houde walter, Joseph S Hayden (2000). Yb/Er co-doped waveguide lasers in phosphate glass, J. of non cryst. Solids 263,369-381.
- [2] Meena, S.L. (2022). Spectral and Upconversion Properties of Eu^{3+} Doped in Zinc Lithium Cadmium Alumino Borogermanate Glasses, Int. J. of Inn. Res. in Sci., Eng. and Tech., 11(2), 1675-1681.
- [3] Reddy, B. N. K., Sailaja, S., Thyaga rajan, K. and Sudhakar Reddy, B. (2020). study of RE ion doped oxide materials wood head publishing, 293-304.
- [4] Kolavekar, S. B. and Ayachit, N.H. (2019). Synthesis of Praseodymium trioxide doped lead boro tellurite glasses and their optical and physical properties, J. of Materiomics, 5, 455-462.
- [5] Kaur, A., Khanna, A. and Aleksandrov, L.I. (2017). Structural, thermal, optical and photo luminescent properties of barium tellurite glasses doped with rare earth ions, Journal of Non-Crystalline Solids 476,67-74.
- [6] Meena, S.L. (2022). Spectral and FTIR Analysis of Ho^{3+} ions doped Zinc Lithium Tungsten Alumino Bismuth borate Glasses, Int. J. of Eng. And Sci. Inv., 11(6), 57-63.
- [7] Rao, V.R. and Jayasankar, C.K. (2019). Spectroscopic investigation on multi-channel visible and NIR emission of Sm^{3+} doped alkali-alkaline earth fluoro phosphate glasses, Opt. Mater. 91,7-16.
- [8] Kashif, I., Ratep, A. and Ahmed, S. (2020). Spectroscopic properties of lithium borate glass containing Sm^{3+} and Nd^{3+} ions, Int. J. of Adv. in App. Sci. 9(3), 211-219.
- [9] Kumar, G.R. and Rao, C.S. (2020). Influence of Bi_2O_3 , Sb_2O_3 and Y_2O_3 on optical properties of Er_2O_3 -doped $CaO-P_2O_5-B_2O_3$ glasses, Bull. Mater. Sci. 43:71, 1-7
- [10] Yasukevich, A. S., Rachkovskaya, G.E., Zakharen, G.B., Trusova, E.E., Kornienko, A. A., Dunina, E.B., Kisel, V. E. and Kuleshov, N. V. (2020). Spectral luminescence properties of oxyfluoride lead silicate germanate glass doped with Tm^{3+} ions, Journal of luminescence, 117667.
- [11] Yaacob, S.N.S., Sahar, M.R., Sazali, E.S., Mahraz, Z. A., Sulhadi, K., Mahraz, Z.A. and Sulhadi, K. (2018). Comprehensive study on compositional modification of Tb^{3+} doped Zinc phosphate Glass, Solid State Sciences 81,51-57.
- [12] Deepa, A. V., murygasen, Priya, Muralimanohar, P., Sathyamoorthy, K. and Vinothkumar, P. (2019). A comparison on the structural and optical properties of different rare earth doped phosphate glass, Optik, 181,361-367.
- [13] Shikerkar, A.G., Desa, J.A.E., Krishna, P.S.R. and Chitr, R. (2000). Diffraction studies of rare earth phosphate glasses, J. of Non-crystalline solids, 270,234-246.
- [14] Mandal, P., Chowdhary, S. and Ghosh, S. (2019). Spectroscopic characterization of Er^{3+} doped lead zinc phosphate glass via Judd- Ofelt analysis, Bulletin of Materials Science 42.
- [15] El Maaref, A.A., Badr, S., Shaaban, Kh.S., Abdel Wahab, E.A. and Elokr, M.M. (2019). Optical properties and radiative rates of Nd^{3+} doped zinc- sodium phosphate Glasses, Journal of rare Earth, 37, 253-259.
- [16] Meena S.L. (2021). Spectral and Transmittance properties of Ho^{3+} ions doped Zinc Lithium Lead Calcium Borophosphate Glasses, 10(9), 50-56.
- [17] Lemiere, A., Bondzior, B., Aromäki, I. and Petit, L. (2022). Study of visible, NIR, and MIR spectroscopic properties of Er^{3+} -doped tellurite glasses and glass-ceramics, J. Am. Ceram Soc., 105, 7186-7195.
- [18] Zhang Y, Xia L, Li C, Ding J, Li J and Zhou X. (2021). Enhanced 2.7 μm mid-infrared emission in Er^{3+}/Ho^{3+} co-doped tellurite glass. Opt Laser Technol. 138:106913.
- [19] Aouaini, F., Maaoui, A., Mohamed, N.B.H., Alanazi, M.M. and El Maati LA. (2022). Visible to infrared down conversion of Er^{3+} doped tellurite glass for luminescent solar converters. J Alloys Compd. 894:162506.
- [20] Romanowski, W. R., Komar J. and Lisiecki, R. (2022). Examining the Spectroscopic and Thermographic Qualities of Er^{3+} -doped Oxyfluoride Germanotellurite Glasses, Materials, 15, 2-14.
- [21] Gorller-Walrand, C. and Binnemans, K. (1988). Spectral Intensities of f-f Transition. In: Gshneider Jr., K.A. and Eyring, L., Eds., Handbook on the Physics and Chemistry of Rare Earths, Vol. 25, Chap. 167, North-Holland, Amst., 101.
- [22] Sharma, Y.K., Surana, S.S.L. and Singh, R.K. (2009). Spectroscopic Investigations and Luminescence Spectra of Sm^{3+} Doped Soda Lime Silicate Glasses. Journal of Rare Earths, 27, 773.
- [23] Judd, B.R. (1962). Optical Absorption Intensities of Rare Earth Ions. Physical Review, 127, 750.
- [24] Ofelt, G.S. (1962). Intensities of Crystal Spectra of Rare Earth Ions. The Journal of Chemical Physics, 37, 511.
- [25] Sinha, S.P. (1983). Systematics and properties of lanthanides, Reidel, Dordrecht.
- [26] Krupke, W.F. (1974). IEEE J. Quantum Electron QE, 10, 450.



10.22214/IJRASET



45.98



IMPACT FACTOR:
7.129



IMPACT FACTOR:
7.429



INTERNATIONAL JOURNAL FOR RESEARCH

IN APPLIED SCIENCE & ENGINEERING TECHNOLOGY

Call : 08813907089  (24*7 Support on Whatsapp)